Talanta 105 (2013) 192–203

Contents lists available at SciVerse ScienceDirect

Talanta

journal homepage: www.elsevier.com/locate/talanta

Identification of phenolic compounds in *Equisetum giganteum* by LC–ESI-MS/MS and a new approach to total flavonoid quantification

Leandro N. Francescato [a,*], Silvia L. Debenedetti [b], Thiago G. Schwanz [c], Valquiria L. Bassani [a], Amélia T. Henriques [a]

[a] Programa de Pós-Graduação em Ciências Farmacêuticas, Faculdade de Farmácia, Universidade Federal do Rio Grande do Sul, Av. Ipiranga 2752, 90610-000 Porto Alegre, RS, Brazil
[b] Facultad de Ciencias Exactas y Naturales, Universidad de Belgrano, C1426DQG, Buenos Aires, Argentina
[c] Núcleo de Análises e Pesquisas Orgânicas–NAPO, Departamento de Química, Universidade Federal de Santa Maria, 97105-900 Santa Maria, RS, Brazil

ARTICLE INFO

Article history:
Received 28 August 2012
Received in revised form
26 November 2012
Accepted 26 November 2012
Available online 2 December 2012

Keywords:
Equisetum giganteum
LC-MS/MS
Flavonoids
Styrylpyrones
Aglycones
Total flavonoid determination

ABSTRACT

Equisetum giganteum L., commonly called "giant horsetail", is an endemic species of Latin America. Its aerial parts have been widely used in ethnomedicine as a diuretic and in herbal medicine and food supplements as a raw material. The phenolic composition of *E. giganteum* stems was studied by liquid chromatography coupled to diode array detection (LC–DAD) and liquid chromatography coupled to electrospray ionization-tandem mass spectrometry (LC–ESI-MS/MS), which identified caffeic acid derivatives, flavonoids and styrylpyrones. The most abundant glycosilated flavonoids in this sample were kaempferol derivatives. Other rare phenolic components, namely, quercetin-3-*O*-(caffeoyl)-glucoside and 3-hydroxy-hispidin-3,4′-di-*O*-glucoside, were reported for first time in the *Equisetum* genus. An LC-UV method for the simultaneous quantification of flavonoid aglycones in *E. giganteum* obtained after hydrolysis was developed and validated. The method exhibited excellent linearity for all analytes, with regression coefficients above 0.998, LOD $\geq$ 0.043 μg mL^{-1}, LOQ $\geq$ 0.158 μg mL^{-1} and recovery rates of 96.89–103.33% and 98.22–102.49% for quercetin and kaempferol, respectively. The relative standard deviation for the intra- and inter-day precision was $\leq$ 3.75%. The hydrolysis process was optimized by central composite rotational design and response surface analysis. The second-order response models for the aglycones contents were as follows: quercetin (μg g^{-1}) = 24.8102 + 55.2823 × HCl + 0.776997 × Time − 7.23852 × HCl^2 − 7.46528E − 04 × Time^2 − 0.229167 × HCl × Time; kaempferol (μg g^{-1}) = −9.66755 + 974.822 × HCl + 11.8059 × Time − 130.612 × HCl^2 − 0.0125694 × Time^2 − 3.22917 × HCl × Time, with estimated optimal conditions of 1.18 M HCl and 205 min of hydrolysis. The results obtained with these new methods were compared to those from a spectrophotometric assay used to determine the total flavonoids in the *Equisetum arvense* monograph (Horsetail, British Pharmacopoeia 2011). For all four species analyzed (*E. giganteum*, *E. arvense*, *E. hyemale* and *E. bogotense*), the calculated aglycone content was higher using the optimized hydrolysis conditions. Additionally, the LC method was more appropriate and specific for quantitative analysis.

1. Introduction

Equisetum giganteum L. (Equisetaceae, subgenus *Hippochaete*), commonly known as "cavalinha", "cola de caballo", "horsetail" or "giant horsetail", is a lower vascular plant widespread in Southern and Central America. This species is used in traditional medicine in Mexico, Guatemala, Venezuela, Argentina and other countries, mainly for its diuretic, astringent, hemostatic and remineralizing properties. It is also used to treat liver and urinary disorders, among other applications [1–5]. In southern Brazil and Argentina, *E. giganteum* infusions are often used as a diuretic and for weight loss. The in vivo diuretic activity of the extracts of this species has been verified [3,4], and no oral acute toxicity was observed in mice [1].

In Brazil and Argentina, the drug is widely used and commercialized as a raw material for herbal medicines and as a food supplement. In these and other Latin American countries, *E. giganteum* is commonly used as a substitute for *E. arvense* (Horsetail herb, Equiseti herba), a European species with confirmed diuretic activity and a long history of clinical use as well as a well-known phytochemical profile [6,7]. Moreover, several pharmacopoeias include monographs of *E. arvense*. In the case of *E. giganteum*, the only known data about its chemical composition have been obtained from metal and silica content analyses, ash determination [5] and oleoresin analysis employing gas chromatography–mass spectrometry [8]. No data on its phytochemical composition have been published.

Considering the wide use of these plants as a raw material in herbal medicine, it is necessary to develop reliable quality control

* Corresponding author. Tel.: +55 51 3308 5258; fax: +55 51 3011 5050.
E-mail address: leandrofrancescato@yahoo.com.br (L.N. Francescato).

0039-9140/$ - see front matter © 2012 Elsevier B.V. All rights reserved.
http://dx.doi.org/10.1016/j.talanta.2012.11.072

methods to comply with regulatory requirements. For this purpose, the pharmacognostic parameters for *E. giganteum* have been examined [9]. Thus, the aim of this study was to determine, for the first time, the phenolic profile of *E. giganteum* using liquid chromatography coupled with tandem mass spectrometry (LC–MS/MS) and to develop and validate a liquid chromatography coupled with ultraviolet detection (LC–UV) method for the quantitation of flavonoid aglycones, including a previous statistical optimization of the acid hydrolysis of their glycosides. Four *Equisetum* species were evaluated: *E. giganteum*, *E. arvense*, *E. hyemale* and *E. bogotense*. The results obtained using this method were compared to those obtained using the hydrolysis and spectrophotometric method described for *E. arvense* in the British Pharmacopoeia 2011 [10].

2. Materials and methods

2.1. Plant material

The aerial sterile stems of *Equisetum giganteum* L. were collected in Santo Antônio da Patrulha (RS, Brazil) in May 2011 (sample 1) and October 2009 (sample 2) [9]. *E. hyemale* L. was collected in August 2009 in Curitiba (PR, Brazil). *E. bogotense* H.B.K. was collected in August 2008 in Bariloche (Río Negro, Argentina). A commercial sample of *E. arvense* L. was purchased in Spain, having been bottled in July 2008. All samples were identified botanically. The material was dried and ground to a particle size < 0.355 mm. Loss on drying was determined at 105 °C for 4 h.

2.2. Chemicals and reagents

Distilled water and analytical-grade reagents were employed in the spectrophotometric and hydrolysis experiments: 37% hydrochloric acid from Quimex (SP, Brazil) and methanol, ethyl acetate and anhydrous sodium sulfate from Synth (SP, Brazil). Ethanol (95%, Synth, SP, Brazil), ultra-pure water (Millipore, MA, USA) and HPLC-grade acetonitrile, methanol and formic acid 96% (Tedia, OH, USA) were used for chromatographic analysis.

Analytical-grade standards of quercetin (Janssen Chimica, Belgium), kaempferol (Chromadex, CA, USA) and astragalin (97%, Sigma-Aldrich, MO, USA) were used as reference compounds.

2.3. LC–MS/MS and LC–DAD qualitative analysis

2.3.1. Sample preparation

The powdered material of *E. giganteum* (0.4 g, sample 1) was extracted with 2 mL of 50% aqueous ethanol (v/v) for 30 min by sonication, centrifuged (1500g) and filtered (0.22 μm PVDF, Millipore, MA, USA). The obtained extract was diluted with ultrapure water (1:5) prior to use in LC–DAD and LC–MS analysis.

2.3.2. Instruments

LC-MS/MS analysis was performed on an Agilent 1200 series HPLC (Palo Alto, CA, USA) equipped with a G1312B SL binary pump, a G1367D high-performance auto-sampler (HiP ALS SL+) and a G1316B SL thermostated column compartment. The mass spectrometer was an Agilent model G6460A triple quadrupole instrument equipped with an electrospray ionization source. Instrument control, data acquisition and processing were performed using MassHunter workstation software (Qualitative Analysis, version B.03.01, Agilent). A Phenomenex Luna C18(2) column (250×4.6 mm^2 i.d., 5 μm particle; Torrance, CA, USA) was used.

A Waters Alliance 2690 Chromatograph Separations Module equipped with a multiple-UV-wavelength photo-diode array detector (Model 996, Waters, Milford, MA, USA) was used for liquid chromatography coupled to diode array detection (LC–DAD) analysis. UV spectra were recorded in a range of 210–400 nm and monitored at 254 nm. Instrument control and data acquisition were performed using Waters Empower Software 2002.

2.3.3. LC–MS/MS and LC–DAD conditions and parameters

Samples were eluted with a gradient of previously degassed 0.3% (v/v) formic acid in water (eluent A, pH 2.2) and acetonitrile (eluent B). The gradient profile was 9–15% B (0–21 min), 15–22% B (21–45 min), 22–35% B (45–60 min), 35–90% B (60–65 min) and 90% B (65–70 min). Separation was carried out at a flow rate of 0.9 mL min^{-1} at 30 °C and the injection volume was 10 μL. Mass spectra of the column eluate were recorded in the range *m/z* 100–1000. The instrument was operated with a capillary voltage of 3500 V and a nozzle voltage of 500 V. Nitrogen was used as the nebulizer gas at 45 psi, a carrier gas of 6 L min^{-1} at 350 °C and a sheath gas of 11 L min^{-1} at 350 °C. MS data were acquired in negative and positive ionization modes for the accurate determination of the *m/z* of the parent ions. MS/MS data were acquired in negative ionization mode to obtain the *m/z* of the fragment ion. For structural interpretation, the MS/MS fragment ions were acquired using different collision-induced decomposition energies (CID) of 10, 20, 30, 50 and 70 V with a fragmentor voltage of 135 V. The classical nomenclature proposed by Domon and Costello [11] in the MS/MS spectra of glycosides was adopted to name the fragment ions.

For LC–DAD analysis, the same chromatographic parameters described for LC-MS/MS analysis were employed, with the exception of an injection volume of 15 μL.

2.4. LC–UV quantitative analysis

2.4.1. Preparation of standard and sample solutions for LC–UV method validation

Quercetin and kaempferol standards were dissolved in methanol and diluted to give seven concentrations in the range of 0.175–43.7 μg mL^{-1} and 0.222–55.6 μg mL^{-1}, respectively. *E. giganteum* (sample 2) was hydrolyzed in 1.8 M HCl for 120 min, extracted and dissolved in methanol according the conditions described below (2.4.5).

2.4.2. Instruments

For the quantitative determination, LC–UV analysis, a Waters Alliance 2695 Chromatograph Separations Module equipped with a UV/VIS detector (Model 2487, Waters) was used. The Luna C18(2) column (4.6×250 mm^2, 5 μm, Phenomenex, CA, USA) was protected by a Bondapak C18 guard-column (1×8 mm^2, 37–55 μm, Waters, MA, USA). To evaluate the specificity, a multiple-UV-wavelength photo-diode array detector (Model 996, Waters) was also used. Empower Software 2002 (Waters) was used for instrument control, data acquisition and processing of the chromatographic information.

2.4.3. LC–UV conditions and parameters

The separation of aglycones was achieved using a linear gradient of water (A) and methanol (B), both acidified with 0.3% formic acid (v/v). The gradient profile was 47–60% B (0–15 min), 60% B (15–23 min), 60–100% B (23–24 min) and 100% B (24–27 min). At the end of each analysis, the column was stabilized for 10 min under the initial conditions. A volume of 10 μL of the sample was eluted with a flow rate of 0.9 mL min^{-1} and detected at 370 nm; the column temperature was 22 ± 2 °C.

2.4.4. LC–UV method validation

The method linearity, precision (repeatability and intermediary precision), accuracy (recovery), specificity, detection and quantitation limits were evaluated according to the ICH guidelines [12].

Linearity: Linearity was determined by the calibration curves obtained from the LC analysis of the standard solutions of quercetin and kaempferol. The linearity analysis, over a 3 day period, was estimated by regression using the least squares method. Seven concentrations of quercetin and kaempferol in the range of 0.175–43.7 $\mu g\ mL^{-1}$ and 0.222–55.6 $\mu g\ mL^{-1}$, respectively, were employed.

Accuracy: The accuracy was determined by recovery analysis. Measured amounts of quercetin (0.091, 0.272 and 0.453 $\mu g\ mL^{-1}$) and kaempferol (1.08, 3.24 and 5.4 $\mu g\ mL^{-1}$) were added to the hydrolyzed extract solution to create solutions with 80, 100 and 120% of the theoretical concentration. Each sample was injected three times and the amount recovered was calculated. Controls from all samples were prepared and analyzed.

Precision: To evaluate the repeatability and intermediate precision (intra- and inter-day precision), five concentration levels (50 to 150%) of the hydrolyzed extract were prepared and injected in triplicate on three different days. A new sample solution was prepared each day. The results were expressed as relative standard deviation (RSD, %).

Specificity: The specificity was determined by peak purity tests using a diode array detector after adding a small amount of the standard substances to the sample.

Limit of detection and limit of quantitation: The limit of detection (LOD) and limit of quantitation (LOQ) were defined as signal-to-noise ratios of 3.3:1 and 10:1, respectively. The standard solutions of quercetin and kaempferol for LOD and LOQ were prepared by sequential dilution.

Robustness: A Plackett–Burman (P–B) design was employed to test the robustness of the method. Four factors were tested: column (two batch and age), formic acid concentration (0.28, 0.3 and 0.32%, v/v), percentage of MeOH in the initial mobile phase composition (46, 47 and 48%) and flow rate (0.85, 0.9 and 0.95 mL min^{-1}). Eight experiments were evaluated with 3 factors assigned to dummy factors, in triplicate and randomly. Three responses were evaluated: the area, retention time and width of the quercetin and kaempferol peaks. The analyses of the results and statistical interpretations of the effects were derived from the literature [13]. The standard error was obtained from the dummy effects. A response at the 5% level ($\alpha=0.05$) was considered significant.

2.4.5. Hydrolysis and extraction

Powdered *E. giganteum* (0.4 g of sample 2) was refluxed in a water bath at 90 ± 1 °C with 40 mL of various final molar concentrations of HCl in 50% aqueous methanol for different time-periods (see next subsection). The liquid was filtered through cotton, and the residue was extracted twice with methanol (10 mL) under reflux (90 ± 1 °C) for 10 min. The extracts were combined, and the methanol was removed at reduced pressure (30–35 °C). Ten milliliters of water were added to the residue and extracted once with 20 mL and then three times with 10 mL of ethyl acetate. The combined ethyl acetate extracts were washed twice with 50 mL of water and then filtered over 10 g of anhydrous sodium sulfate. The resulting solution was dried at reduced pressure (<40 °C). The residue was resuspended in 5 mL of methanol, 5-fold diluted in the same solvent and filtered through a 0.45 μm PVDF filter (Millipore, MA, USA) prior to LC analysis.

2.4.6. Experimental design and optimization of hydrolysis by response surface methodology (RSM)

The acid hydrolysis of the *E. giganteum* raw material was optimized using central composite rotational design (CCRD) and response surface analysis [14,15] to maximize its efficiency while avoiding the degradation of the flavonoid aglycones.

According to results obtained in preliminary research on the efficiency of the acid hydrolysis of flavonoid glycosides, the most relevant variables were identified as the HCl concentration and hydrolysis time. CCRD was developed using Minitab® 15.0 Statistical Software (Minitab Inc., USA). Twelve experiments were performed in two orthogonal blocks with 2 center points per block. The values of the variables were coded as ±1 for the factorial points, 0 for the center points and ±1.4142 for the axial points. The ranges of the variables evaluated were 1.02 to 4.98 M for HCl concentration and 35.1 to 204.9 min for hydrolysis time (see Table 4).

The experimental data were fitted in the second-order polynomial model encoded in

$$Y = b_0 + b_1X_1 + b_2X_2 + b_{11}X_1^2 + b_{22}X_2^2 + b_{12}X_1X_2 \quad (1)$$

where Y is the response variable to be modeled; b_0, b_1, b_2, b_{11}, b_{22} and b_{12} are the regression coefficients; X_1 is the molar concentration of HCl; and X_2 is the hydrolysis time.

The suitability of the model for each extracted flavonoid aglycone was verified by analysis of variance (ANOVA). The optimum HCl concentration and hydrolysis time were obtained from the model by inspecting the response surface contour plots and using the Minitab® optimizer. The determination of flavonoid aglycones was carried out by LC–UV after hydrolysis at the optimum conditions, and the result was compared to the predicted value.

2.5. Statistical analysis

Analyses were performed in triplicate. The individual data were grouped after each experiment. The mean with the respective deviation was used as a measurement of the central tendency and dispersion (RSD, %). Microsoft Excel software (Microsoft, USA) and Minitab® 15.0 Statistical Software (Minitab Inc., USA) were employed for ANOVA.

3. Results and discussion

3.1. Qualitative analysis

The LC-DAD and LC–ESI-MS profiles of *E. giganteum* hydroethanolic extract are shown in Fig. 1, and the chromatographic, UV, MS and MS/MS data can be observed in Table 1.

The molecular mass of the compounds was obtained from their positive and negative ion electrospray mass spectra (ESI-MS), which described the corresponding protonated and deprotonated pseudomolecular ions as well as the sodium and potassium adduct ions (Table 1). In some cases, sodium formate adduct ions ($[M+68]^-$ and $[M+136]^-$), formed due to the presence of formic acid in mobile phase A (data not shown) were observed in the negative ion mode ESI-MS. After the pseudomolecular ion identification, it was subjected to various CID energies (10, 20, 30, 50 and 70 V) in negative ion mode ESI-MS/MS to detect the site of substitution in the aglycones, thereby providing firm evidence for the proposed compound structure.

Thus, the structure of 12 compounds present in hydroethanolic extract of *E. giganteum* were fully or partially characterized using the combined interpretation of the retention time, UV spectra and fragmentation patterns of the compounds obtained by LC–DAD and LC–ESI-MS/MS. These data were compared with

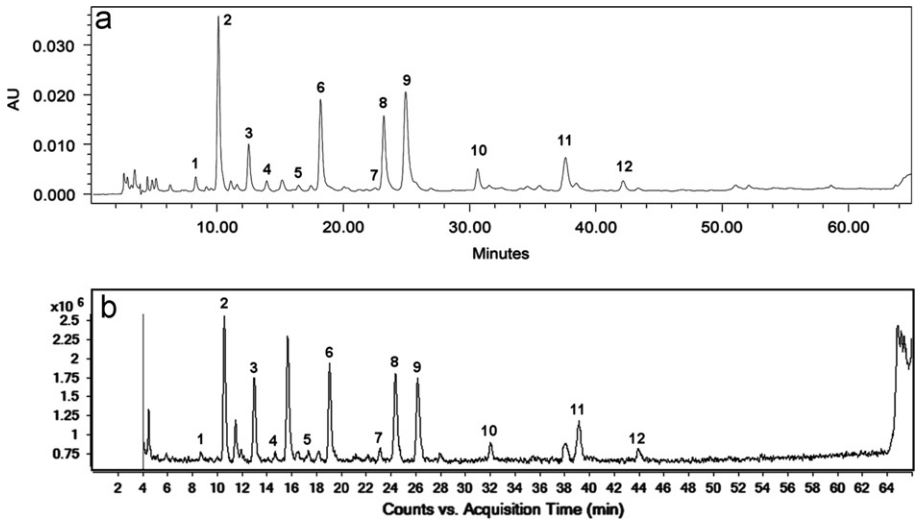

Fig. 1. LC–DAD chromatogram at 254 nm (a) and LC–ESI-MS (negative ion mode) total ion current (TIC) chromatogram (b) of the hydroethanolic extract of *E. giganteum*. The peaks are labeled according to the compounds listed in Table 1.

literature data, mainly those for the phenolics present in other *Equisetum* species [7,16–18].

3.1.1. Characterization of flavonoid derivatives

In combination with the application of different CID energies in negative ion mode ESI-MS/MS, the UV spectral data were used to characterize the site of substitution in the flavonoid aglycone. Band II is important for the identification of hydroxyl or methoxyl substituents in the ring B, and hypsochromic shifts in Band I and/or II can indicate the methylation or glycosidation of the hydroxyl groups of flavonols [19]. Shoulders in the UV spectra can also indicate substitution in aglycones: kaempferol (266, 294sh, 349 nm for 3-glycosides and 266, 318sh, 349 nm for 3,7-diglycosides) and quercetin (255, 266sh, 355 nm for 3-glycosides and 255, 266sh, 294sh, 354 nm for 3,7-glycosides) [20].

Four peaks (compounds 2, 6, 10 and 12) had UV spectra compatible with kaempferol glycosides. The UV spectra of compounds 2 and 6 showed a Band I maximum at 346.5 nm and a shoulder at 318 nm, indicating 3,7-*O* substitution. In contrast, the UV of the compounds 10 and 12 showed a Band I maximum at 344.1 nm and a shoulder at 290 nm, indicating a 3-*O* substitution [19,20].

The Y_0^{7-} [M-H-162]$^-$ at *m/z* 609 (compound 2, [M-H]$^-$ of *m/z* 771.1 amu) and *m/z* 447 (compound 6, [M-H]$^-$ of *m/z* 609 amu) were the base peak at 20 and 30 V of CID energy, indicating the loss of a glucose residue at the 7-*O* position, which is preferential [20]. For compound 2 (at 30 V), the ion $^{0,2}X_0^-$ [M-H-120]$^-$ at *m/z* 651.2, with low intensity (0.6%), and the ion $Y_0^7Z_1^{3-}$ [M-H-342]$^-$ at *m/z* 428.7 (1.6%) (Table 1) indicated the 1→2 interglucosidic linkage and breakdown of a sugar moiety with the loss of one glucose residue, respectively, which are characteristic of the flavonoid 3-*O*-sophoroside. The ion *m/z* 445.8 indicated the flavonoid 3- or 7-*O*-glucosyl, and the ion with *m/z* 284.8 indicated the aglycone, kaempferol [21]. For compound 6, the characteristic ion Z_1^- [M-H-180]$^-$, indicating 1→2 interglycosidic linkage, was not detected. The ions $^{0,2}X_0^-$ [M-H-120]$^-$ at *m/z* 488.9 and [M-H-282]$^-$ at *m/z* 327 indicated breakdown with partial loss of a hexose residue. The $Y_0^{3,7-}$ [M-H-324]$^-$ ion at *m/z* 284 indicated kaempferol [21]. The homolytic cleavage of the 3,7-*O*-glycosidic bond in compounds 2 (at 70 V) and 6 (at 50 V) produced the radical aglycone ions $[Y_0\text{-}2H]^{\bullet-}$ *m/z* 283 (base peak) and $[Y_0\text{-}H]^{\bullet-}$ *m/z* 284 as well as the aglycone $[Y_0]^-$ ion *m/z* 284.9/ 285, indicating a di-*O*-glycoside [22,23]. The ions *m/z* 255/254.8 and 226.8/226.6, for compound 2 and 6, respectively, confirmed kaempferol [24], whereas the ion *m/z* 151.2/150.6 indicated the presence of a 7-*O*-glucoside [25]. Thus, compound 2 was identified as kaempferol-3-*O*-sophoroside-7-*O*-glucoside and compound 6 as kaempferol-3,7-di-*O*-glucoside. The influence of increasing fragmentation energy (CID) on the fragmentation pattern of compound 2 can be visualized in Table 1 and Fig. 2.

For compound 10 ([M-H]$^-$ of *m/z* 609 amu), the base peak Y_0^{3-} [M-H-325]$^-$ at 30 V indicated the loss of a diglucose residue and the kaempferol deprotoned aglycone at *m/z* 284. The characteristic ion Z_1^- [M-H-180]$^-$ at *m/z* 428.9 indicated the 1→2 interglycosidic linkage of the flavonoid sophoroside. For compound 12 ([M-H]$^-$ of *m/z* 447 amu), the Y_0^{3-} [M-H-163]$^-$ (base peak at 30 V) indicated the loss of a glucose residue and kaempferol at *m/z* 283.9. The ion $^{0,2}X_0^-$ [M-H-120]$^-$, indicating the loss of a sugar residue, was only detected at 20 V [21]. For compounds 10 and 12, the homolytic cleavage of the 3-*O*-glycosidic bond produced more intense radical aglycone $[Y_0\text{-}H]^{\bullet-}$ ions *m/z* 284 and 283.9 than the aglycone $[Y_0]^-$ ions *m/z* 284.9 and 284.8, respectively, confirming the glycosylation site at 3-*O* position [22,23]. The ions *m/z* 255 and 227, formed in MS/MS at 50 and 70 V for compound 10 and 30 and 50 V for compound 12, respectively, are characteristic of kaempferol [24]. The ion *m/z* 151, characteristic of kaempferol-7-*O*-glucoside, was not detected for either compound [25]. Compound 10 was identified as kaempferol-3-*O*-sophoroside, and compound 12 was unambiguously identified as astragalin (kaempferol-3-*O*-glucoside) based on a comparison of the retention times and MS and MS/MS spectra with those of a reference compound.

Compound 1 and 4 exhibited UV spectra characteristic of a quercetin derivative. The Band I maximum at 351.3 and 348.9 nm and the shoulder at 294 nm of compound 1 and 4 indicated a 3,7-*O* substitution. The characteristic ions Z_1^- and $^{0,2}X_0^-$ of 1→2 interglycosidic linkages were not detected [21] for either flavonoid. The presence of ions at *m/z* 300.5 and 300.8 at 30 V, in addition to the fragment ions at *m/z* 271 and 270.9 at 70 V for compound 1 and 4, respectively, indicated the aglycone quercetin [24].

The fragmentation pattern of compound 1 ([M-H]$^-$ of *m/z* 787 amu) indicated the presence of 3 hexoses linked to the aglycone by two or three *O*-glycosidic linkages. At 30 V, the [M-H]$^-$ ion *m/z* 787 was the base peak, followed by the [M-H-162]$^-$ ion *m/z* 625 (34.2% R.A.), [M-H-325]$^-$ ion *m/z* 462 (30.7%) and [M-H-487]$^-$ ion *m/z* 300.5 (3.7%), making it difficult to infer the location of the substitution from the relative abundances. At 50 V, the base peak was the ion *m/z* 462, indicating that there is a hexose residue possibly linked at 3-*O* position (the

Table 1
Retention time (R_t), UV absorptions (λ_{max}), negative and positive ion mode ESI-MS and negative ion mode ESI–MS/MS data of phenolic compounds presents in hydroethanolic extract of *E. giganteum*.

Compound	R_t (min), LC–DAD (RSD, %)[a]	UV λ_{max} (nm)[b]	Negative ion mode (*m/z*)			Positive ion mode (*m/z*)		Phenolic compound
			MS $[M-H]^-$	CID (V)	MS/MS (R.A. %)	$[M+H]^+$	$[M+Na]^+$ $[M+K]^+$	
1	8.3 (0.84)	253.4, 267sh, 294sh, 351.3	787	10 20 30 50 70	787.1 (100), 625.1 (0.7) 787.1 (100), 624.7 (5.9) 787 (100), 625 (34.2), 462 (30.7), 300.5 (3.7), 242.8 (9) 462 (100), 300 (31), 298.8 (87.8) 299.7 (2.7), 298.9 (100), 271 (16.4), 150.6 (2.1)	789.1	811.3 827.2	Quercetin-tri-*O*-hexoside
2	10.1 (0.32)	265.2, 318sh, 346.5	771.1	10 20 30 50 70	771.1 (100), 609.1 (59.3), 607.9 (0.4), 284 (0.4) 771.1 (13.6), 609.2 (100), 284.8 (0.2), 284.1 (0.4) 770.7 (0.4), 651.2 (0.6), 609 (100), 445.8 (3.1), 428.7 (1.6), 284.8 (2.5), 284 (3.6), 282.3 (0.4), 178.6 (0.3) 609.1 (7.9), 446 (19.4), 428.9 (5.8), 325.9 (2.2), 285 (42.5), 284 (100), 282.9 (43.1), 254.8 (5.3), 179.1 (1.8), 178.6 (1.4), 151 (2.4) 309.1 (0.6), 284.9 (29.5), 284 (49.9), 283 (100), 256.9 (1.7), 255.9 (1.7), 255 (61.2), 226.8 (12.9), 181.7 (0.8), 151.2 (1.9)	773.3	795.2 811.2	Kaempferol-3-*O*-sophoroside-7-*O*-glucoside
3	12.5 (0.30)	253.4, 268sh, 361.8[c]	585.1	10 20 30 50 70	585.1 (100), 422.9 (4.2) 585.0 (100), 423.1 (21.2), 422 (2.8), 259.8 (2.5), 259.1 (1.9), 241 (2), 217.2 (2.7), 215.9 (2.2), 202.8 (2.4) 585 (63.6), 423.1 (100), 422.1 (26.7), 379.1 (14.1), 259.9 (90.3), 259 (96.4), 257.8 (6.5), 230.8 (28), 217 (41.7), 216 (44.8), 214.9 (6.3), 202.9 (52.3), 159 (6.9) 259.5 (10.1), 259 (8.4), 216.9 (11.5), 215.9 (10.6), 202.9 (100), 188 (7.6), 186.7 (19), 174.3 (7.8), 171 (5.1), 159 (60.2), 142.4 (6.4) 203 (19.9), 186.9 (6.9), 175.3 (3.7), 172.8 (3.2), 170.8 (8.9), 159 (100)	587.2	609.2 625.2	3-Hydroxyhispidin-3, 4′-di-*O*-glucoside
4	13.9 (0.66)	253.4, 267sh, 294sh, 348.9	625.1	10 20 30 50 70	625 (100), 462.9 (6.1) 625.1 (100), 462.8 (31.3), 461.8 (4.6) 624.5 (6.9), 463 (31.5), 462 (100), 300.8 (29.3), 299 (11.7) 301 (10.3), 299.9 (3.9), 298.8 (100), 270.9 (3.2) 300.8 (10.7), 298.6 (48.6), 270.9 (100), 243.1 (4.1), 242.2 (5.3)	627.3	649.2 665.1	Quercetin-3,7-di-*O*-glucoside
5	16.5 (0.73)	246.2, 295sh, 327.3	625.1	10 20 30 50 70	624.9 (100), 462.9 (42.4) 624.8 (10.3), 463.1 (100), 462.4 (42.1), 341.5 (13.5) 463.1 (100) 300.8 (46.8), 300.1 (72.5), 270.9 (100), 255.1 (99), 227.1 (30.4) 270.6 (93.3), 254.7 (84.1), 242.6 (100)	627.1	649.2 665.0	Quercetin-3-*O*-(caffeoyl)-glucoside
6	18.2 (0.85)	265.2, 318sh, 346.5	609	10 20 30 50 70	609 (100), 489.2 (0.6), 488.8 (0.5), 447 (12.4), 446 (1.1), 285 (0.4), 282.9 (0.5) 609.1 (65.2), 489.1 (6.8), 447 (100), 445.8 (9.4), 285.1 (23.4), 282.8 (1.5) 609.2 (1.6), 488.9 (2.3), 460.1 (1.1), 447 (100), 446 (77). 327 (4), 285 (85.8), 283.9 (3.6), 283 (24), 269.2 (1), 255.1 (2), 151 (0.9) 446.7 (0.7), 445.9 (0.5), 297.2 (0.6), 285 (60.5), 284 (11), 283 (100), 254.8 (13.8), 226.6 (2.2), 150.6 (1.1) 284.9 (18.5), 282.9 (44.3), 254.9 (100), 227.1 (10.2), 183 (5.3)	611.2	633.2 649.2	Kaempferol-3,7-di-*O*-glucoside
7	22.2 (0.64)	267.6, 353.5	625	10 20 30 50 70	625.1 (100) 625.2 (58.1), 624.6 (100), 463.2 (8.1) 625.1 (34.5), 624.6 (35), 463 (100), 462.2 (19.4), 461.5 (7), 299.9 (5.6) 300.4 (22.5), 299.9 (18.3), 299 (64.2), 271.1 (100), 254.8 (25.6), 201.1 (10.4) 270.7 (84.2), 255.2 (100), 254.6 (95.2), 227 (21.1)	627.2	649.2 665.2	Flavonol-di-*O*-hexoside
8	23 (0.73)	253.4, 272sh, 371.4	423	10 20 30 50 70	423 (100), 379.1 (1.8), 378.4 (0.8), 286.9 (1.2), 261 (8.6), 260 (1.5), 217 (1.1), 215.9 (0.8) 423 (100), 261.1 (62.7), 260.1 (49.2), 216.9 (32.3), 216 (25.5), 202.9 (49.5), 198.8 (8), 189.2 (8), 188.1 (17), 172.9 (7.6), 161 (6.9), 159 (4.9), 135 (8.8), 127.1 (5.6) 260.9 (14.4),259.7 (12.5), 216.9 (24.7), 216.1 (6.1), 215.5 (10.7), 202.8 (100), 197.3 (6.7), 188 (18.7), 187 (13.1), 174.1 (6.1), 172.8 (11.2), 172.1 (6.7), 161.1 (7.3), 159 (22.4), 135.1 (14) 202.8 (100), 186.9 (34.4), 175 (7.3), 171.1 (4.4), 159 (41), 158 (4.9), 144 (7.8), 135 (15.5), 108.9 (7.3) 203 (36.6), 186.7 (18.6), 160.8 (11.8), 159.8 (5.5), 159 (100), 135.1 (11.6), 134.3 (12.1), 132.6 (7.3)	425.1	447.1 463.1	Equisetumpyrone

Table 1 (*continued*)

Compound	R_t (min), LC–DAD (RSD, %)[a]	UV λ_{max} (nm)[b]	Negative ion mode (*m/z*)			Positive ion mode (*m/z*)		Phenolic compound
			MS $[M-H]^-$	CID (V)	MS/MS (R.A. %)	$[M+H]^+$	$[M+Na]^+$ $[M+K]^+$	
9	24.9 (0.60)	244, 298sh, 327.3	295	10 20 30 50	201 (52.4), 200.4 (11.8), 179.1 (29.1), 134.9 (7.5), 132.7 (100), 114.6 (8.8) 200.8 (68.9), 178.8 (54.8), 135.2 (100), 134.2 (84.8), 133.2 (83.4), 115 (98.3) 134.9 (80.2), 133.7 (18.6), 115.2 (100) 135 (83.5), 133.6 (100)	–	319.1 335	Caffeic acid derivative
10	30.6 (0.52)	265.2, 290sh, 344.1	609	10 20 30 50 70	609.1 (100), 283.4 (0.4) 609.1 (100), 428.9 (2.1), 285 (5.4), 284.1 (7) 609.1 (14.2), 446.8 (1.3), 428.9 (5.3), 284.9 (15.3), 284 (100), 256.9 (1.6), 178.8 (1.3), 126.8 (1.5) 285 (8.7), 284 (100), 255 (77.5), 228.9 (3.9), 226.9 (51.6) 283.4 (4.6), 255 (100), 227 (60.3), 210.8 (5.1)	611.2	633.2 649.2	Kaempferol-3-*O*-sophoroside
11	37.6 (0.53)	241.5, 298sh, 327.3	309	10 20 30	192.9 (100), 177.6 (7.1), 134.2 (22.5), 133.5 (9.3), 115.1 (10.7) 193.1 (13.1), 192.5 (14.1), 134 (100), 117.1 (9.3) 134.2 (100)	–	333.1 349.2	Ferulic acid derivative
12	42.2 (0.54)	265.2, 290sh, 344.1	447	10 20 30 50 70	447 (100), 284.6 (3.6) 447.1 (100), 326.6 (11.1), 285.2 (38.1), 284.7 (34.9), 283.9 (61.8), 255.2 (7.9), 226.7 (19), 174.6 (16.8) 447 (10.1), 284.8 (6.2), 283.9 (100), 254.8 (52.1), 227 (14.2), 174.7 (13) 256.1 (5.1), 255 (100), 254.5 (37.5), 227 (69.3) 226.8 (100), 211.2 (8), 183.1 (20.7), 181.8 (11.6)	449	471.1 487	Kaempferol-3-*O*-glucoside

[a] Percent relative standard deviation of the triplicate measurements.
[b] Shoulders obtained visually.
[c] Other compound coeluting in the same peak. UV spectra maxima tentatively selected for the compound of interest.

most difficult breakdown position). The homolytic cleavage of the *O*-glycosidic bond produced (at 70 V) radical aglycone ions $[Y_0\text{-}2H]^{\bullet-}$ *m/z* 298.9 (high abundance) and $[Y_0\text{-}H]^{\bullet-}$ *m/z* 299.7 (low abundance), but the aglycone ion $[Y_0]^-$ *m/z* 301 was not observed. The ion $[Y_0\text{-}2H]^{\bullet-}$ indicated the presence of a di-*O*-glycoside [22], but no reference to the absence of an aglycone ion was found in literature. Attributing this peak to the tri-*O*-glycosidic linkage, compound 1 was identified as quercetin-tri-*O*-hexoside.

In compound 4 ($[M\text{-}H]^-$ of *m/z* 625.1 amu), the ion Y_0^{7-} $[M\text{-}H\text{-}162]^-$ (base peak) at *m/z* 462 appears at 30 V, indicating the loss of a hexose residue in the 7-*O* position, which is preferential. The $Y_0^{3,7-}$ $[M\text{-}H\text{-}324]^-$ ion at *m/z* 300.8 indicated quercetin [21]. The homolytic cleavage of the 3,7-*O*-glycosidic bond produced (at 50 V) radical aglycone ions $[Y_0\text{-}2H]^{\bullet-}$ *m/z* 298.8 (high intensity) and $[Y_0\text{-}H]^{\bullet-}$ *m/z* 299.9 as well as the aglycone $[Y_0]^-$ ion *m/z* 301, indicating a di-*O*-glycoside [22]. Thus, compound 4 was identified as quercetin-3,7-*O*-glucoside.

Compound 5 ($[M\text{-}H]^-$ of *m/z* 625.1 amu) had a UV spectra characteristic of a hydroxycinnamic acid, but the fragmentation pattern indicated an *O*-substituted flavonol. At 10 V, only the ion $[M\text{-}H\text{-}162]^-$ *m/z* 462.9 was formed in high intensity after the loss of the caffeoyl moiety from the pseudomolecular ion $[M\text{-}H]^-$ *m/z* 624.8. At 20 V, in addition to the ion *m/z* 463.1 (100%), the ion [M-H-Caf-120] *m/z* 341.5 (13.5%) indicated the breakdown of a sugar moiety. The homolytic cleavage of the *O*-substitute bond produced (at 50 V) a radical aglycone ion $[Y_0\text{-}H]^{\bullet-}$ *m/z* 300.1 (72.5%) as well as the aglycone ion $[Y_0]^-$ *m/z* 300.8 (46.8%), implying a possible 3-*O*-substitution [23]. The ions *m/z* 270.9 and 255.1, formed in MS/MS at 50 V, are characteristic of quercetin [24]. Based on a comparison of the MS fragmentation pattern with the literature [26], compound 5 was identified as quercetin-3-*O*-(caffeoyl)-glucoside.

Compound **7** ($[M\text{-}H]^-$ of *m/z* 625 amu) exhibited a UV spectra typical of a flavonol, and the Band I maximum at 353.5 nm indicated that the compound was 3-*O* substituted. The ion $[M\text{-}H\text{-}162]^-$ at *m/z* 463 (base peak), indicated the loss of a hexose residue. The characteristic ion of a 1→2 interglycosidic linkage was not detected. The $Y_0^{3,7-}$ $[M\text{-}H\text{-}324]^-$ ion at *m/z* 299.9 indicated the aglycone. The homolytic cleavage of the *O*-glycosidic bond produced (at 50 V) radical aglycone ions $[Y_0\text{-}2H]^{\bullet-}$ *m/z* 299 (high intensity) and $[Y_0\text{-}H]^{\bullet-}$ *m/z* 299.9, indicating a di-*O*-glycoside, possibly with 3-*O*-glycosidic linkage [22,23]. The ions *m/z* 271.1 and 254.8, formed in MS/MS at 50 V, indicated the aglycone quercetin [24], whereas the ion *m/z* 227 (at 70 V) corresponds to the MS/MS of kaempferol derivatives. Further research is thus needed to elucidate the structure of this derivative.

3.1.2. Characterization of styrylpyrone derivatives

Compounds 8 and 3 exhibited UV spectra characteristic of styrylpyrone, with maximum in the range of 253–258 nm and 355–373 nm [16].

The results obtained for compound 8 were compared with literature data [7,16,17]. At low collision energy (10 and 20 V) in MS/MS, the aglycone ion *m/z* 261 was detected from the pseudomolecular ion $[M\text{-}H]^-$ *m/z* 423 (base peak), indicating the loss of a hexose residue (β-glucose) $[M\text{-}H\text{-}162]^-$. Thus, compound 8 was characterized as equisetumpyrone, a styrylpyrone glycoside (3,4-dihydroxy-6-(3′,4′-dihydroxy-*E*-styryl)-2-pyron-3-*O*-*β*-D-glucopyranoside). This attribution could be confirmed by the presence of the ions *m/z* 379.1 and 217 at 10 V, which indicated the loss of CO_2 following the opening of the pyrone ring, and the ions *m/z* 159 and 135.1 at 20 V, characteristic of a di-hydroxylated styryl group [16]. The MS/MS fragmentation pattern of compound 8 at 30 V is presented in Fig. 3.

The results obtained for compound 3 were compared with literature data [16], and the compound was initially characterized

as 3-hydroxyhispidin-sophoroside. Our data, however, indicated that the compound was di-*O*-substituted because at low collision energy (10 V) in MS/MS, only the $[M\text{-}H\text{-}162]^-$ ion at *m/z* 422.9, characteristic of 3-hydroxyhispidin-hexoside, was present, corresponding to the loss of a hexose residue. Furthermore, at 30 V, this ion was the base peak and the pseudomolecular ion *m/z* 585 and aglycone ions at *m/z* 259.9 and 259 exhibited high relative abundances (63.5, 89.6 and 96.4% R.A., respectively), which usually occurs in di-*O*-substituted compounds [21]. Moreover, the characteristic ion $[M\text{-}H\text{-}180]^-$, typical of a 1→2 interglycosidic linkage of sophoroside, was not detected with any of the employed collision energies. Fragments at *m/z* 379.1, 216, 202.9 and 159, present in equisetumpyrone spectra, were observed. In the fast atom bombardment mass spectrometry (FAB-MS) spectra presented by Beckert [16], in addition to ions *m/z* 585 and 423, another fragment at *m/z* 325 was reported, which the author attributed to sophoroside (not observed in our experiment). However, that fragment may be due to the cleavage of the pyrone ring and formation of an ion containing a dihydroxy-styryl-*O*-glucoside derivative. Based on these data, compound 3 was identified as 3-hydroxyhispidin-3,4′-di-*O*-glucoside (3,4-dihydroxy-6-(3′,4′-dihydroxy-*E*-styryl)-2-pyron-3,4′-*O*-*β*-diglucopyranoside), although the position of the attachment of the glucose residue to the dihydroxy-styryl group must to be confirmed by NMR analysis.

3.1.3. Characterization of hydroxycinnamic acid derivatives

Two hydroxycinnamic acid esters were identified: compounds 9 and 11. These compounds presented UV spectra characteristic of hydroxycinnamic acid derivatives (with maximum at 324–326 nm and a shoulder at 296 nm) and fragmentation patterns in accordance with those reported for caffeic acid ester derivatives [27], with a high fragmentation tendency even at a low collision energy (10 V). In the negative ion mode ESI-MS, compound 9, beyond the pseudomolecular ion *m/z* 295, an ion indicating a dimeric adduct of the compound $[2M\text{-}H]^-$ *m/z* 591 was observed (data not shown).

Compound 9 was identified as a caffeic acid ester derivative (UV λ_{max}=244, 298sh, 327.3 nm; $[M\text{-}H]^-$ of *m/z* 295 amu). In the MS/MS fragmentation at 20 V, the fragment ion $[M\text{-}116]^-$ *m/z* 178.8 is formed after the ester breakdown of the pseudomolecular ion *m/z* 295. This ion, in turn, yielded the ion $[M\text{-}116\text{-}CO_2]^-$ *m/z* 135.2, characteristic of caffeic acid. Compound 11 was identified as a ferulic acid ester derivative (UV λ_{max}=241.5, 298sh, 327.3 nm; $[M\text{-}H]^-$ of *m/z* 309 amu). In the MS/MS at 10 V, after the ester breakdown with the loss of a residue $[M\text{-}H\text{-}116]^-$, the fragment ion *m/z* 192.9 corresponding to ferulic acid (base peak) is produced. This ion then yielded the ion $[M\text{-}H\text{-}116\text{-}CH_3]^-$ at *m/z* 177.6 after the loss of the methyl of the methoxy group and the ion $[M\text{-}H\text{-}116\text{-}CH_3\text{-}CO_2]^-$ at *m/z* 134.2, indicating the loss of CO_2 of the acid group, all of which are characteristic of a ferulic acid derivative. The fragment with *m/z* 116 present in both compounds could not be identified.

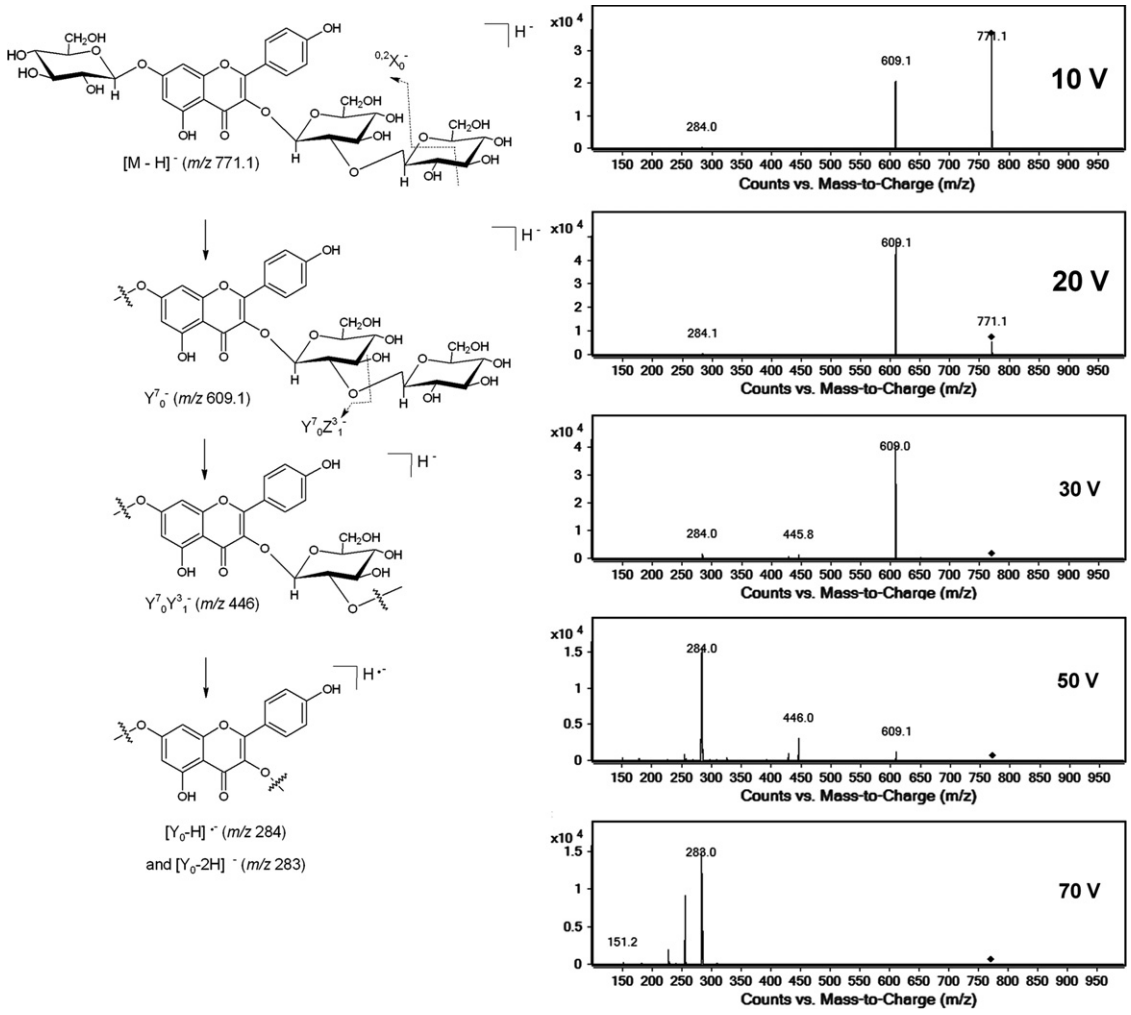

Fig. 2. Principal fragmentation pathway and MS/MS $[M\text{-}H]^-$ at CID energies of 10, 20, 30, 50 and 70 V for compound 2, kaempferol-3-*O*-sophoroside-7-*O*-glucoside.

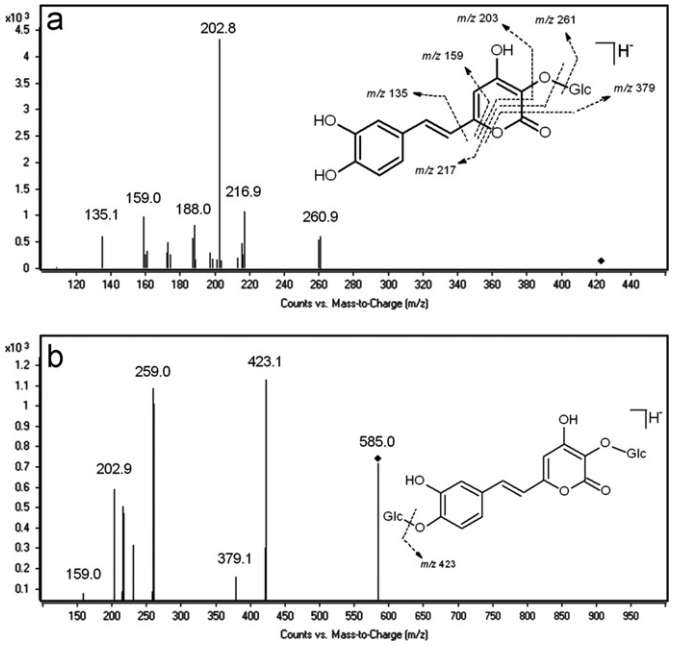

Fig. 3. MS/MS $[M-H]^-$ at 30 V for styrylpyrone derivatives: compound 8, equisetumpyrone (a); compound 3, 3-hydroxyhispidin-3,4′-di-*O*-glucoside (b).

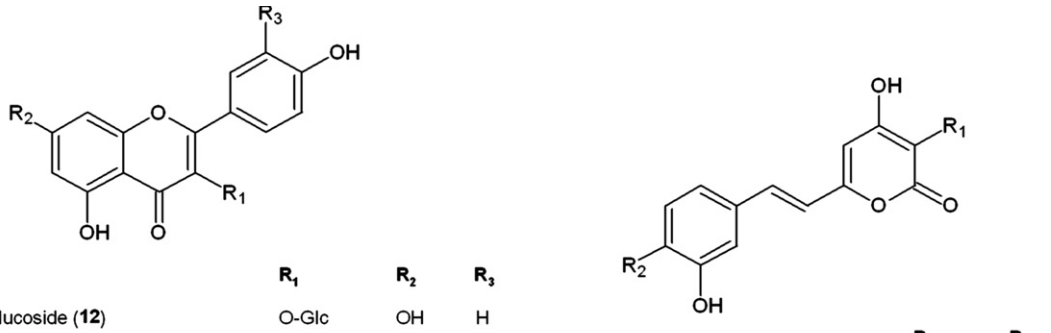

	R_1	R_2	R_3
Kaempferol-3-*O*-glucoside (**12**)	O-Glc	OH	H
Kaempferol-3-*O*-sophoroside (**10**)	O-Soph	OH	H
Kaempferol-3,7-di-*O*-glucoside (**6**)	O-Glc	O-Glc	H
Kaempferol-3-*O*-sophoroside-7-*O*-glucoside (**2**)	O-Soph	O-Glc	H
Quercetin-3,7-di-*O*-glucoside (**4**)	O-Glc	O-Glc	OH
Quercetin-3-*O*-(caffeoyl)-glucoside (**5**)	O-Caff-Glc	OH	OH

	R_1	R_2
Equisetumpyrone (**8**)	OGlc	OH
3-Hydroxyhispidin-3,4'-di-*O*-glucoside (**3**)	OGlc	OGlc

Fig. 4. Structure of the styrylpyrones and flavonols identified by LC–MS/MS and LC–DAD in the hydroethanolic extract of *E. giganteum*.

The pattern of phenolics of *E. arvense* and other European *Equisetum* species is well known: flavonoid *O*-glycosides (mainly apigenin, genkwanin, quercetin and kaempferol derivatives), caffeic acid conjugates (5-*O*-caffeoylshikimic acid, chlorogenic acid, dicaffeoyl-meso-tartaric acid and monocaffeoyl-meso-tartaric acid) and equisetumpyrone [7,28]. Thus, some compounds identified for the first time in *E. giganteum* in this study (Fig. 4) have been previously reported for the genus, whereas other compounds, such as quercetin-3-*O*-(caffeoyl)-glucoside, 3,4-dihydroxy-6-(3′,4′-dihydroxy-*E*-styryl)-2-pyron-3,4′-*O*-*β*-di-glucopyranoside, and caffeic and ferulic acid ester derivatives, are reported for first time in the *Equisetum* genus.

Styrylpyrone glycosides are rare natural products found in a few species of the *Equisetum* genus [7,16,17]. Some of these compounds are found in high levels in the rhizomes, gametophytes and fertile sporophytes of *E. arvense* and may be involved in the constitutive defense mechanism against pathogens [16,29]. However, equisetumpyrone was found as one of the major constituents, together with other di-*O*-hexoside styrylpyrone, in the aerial sterile stems of *E. giganteum*.

The flavonol glycosides and equisetumpyrone characterized in *E. giganteum* and previously described for the *Equisetum* species [7,18] can be employed as chemotaxonomic markers. Among the kaempferol derivatives, the kaempferol-3-*O*-sophoroside was reported for all species found in the references evaluated [7,18,28,30], suggesting its potential use as a marker for the genus.

3.2. Quantitative analysis: flavonoid aglycone determination

As flavonoids are important constituents of *Equisetum* spp. and present many recognized medicinal properties, they can be used as chemical markers for quality control purposes. Chromatographic techniques in combination with UV detection can be used for the reliable quantitation of individual flavonoid glycosides. However, owing to the complexity of many extracts, the absence of many commercial analytical standards, the similarity

Table 2
Calibration curves, LOD and LOQ data of flavonoids aglycones determined by LC–UV.

Compound	Linearity range (μg mL^{-1})	Slope ± standard error	Intercept ± standard error	LOD (μg mL^{-1})	LOQ (μg mL^{-1})	Determination coefficient (R^2)
Quercetin	0.175–43.7	43553.4 ± 93.6	−6580.8 ± 2293.7	0.047	0.158	0.9997
Kaempferol	0.222–55.6	39563.6 ± 197.5	−5752.6 ± 6157.8	0.043	0.205	0.9985

between the spectra of different flavonoids glycosides, the low reproducibility of retention times on long runs (> 50 min) and the possibility of co-eluting compounds, this quantification technique is often difficult to perform. Therefore, quantitative analysis of the flavonoid aglycones, after the hydrolysis of glycosides, is a simpler and faster approach because most aglycones are commercially available as reference compounds. Thus, this method is an attractive alternative appropriate for routine analysis.

Considering the complexity of the plant matrix and the different flavonoid glycosides (i.e., aglycone moiety, *C* or *O*-glycosides bond, substitution position and different types of substituents), the optimization of the hydrolysis process is necessary to ensure its efficacy and accuracy.

For the quantitative analysis of the total flavonoid aglycones in *E. arvense*, the British Pharmacopoeia 2011 (BP2011) [10] employed a colorimetric method, which consists of the acid hydrolysis of the glycosides and their subsequent spectrophotometric determination at 425 nm of a complex formed with $AlCl_3$. Like all methods of this type, it is non-specific and most likely inaccurate if applied to the quantification of flavonoid aglycones obtained in *E. giganteum* because its flavonoid profile is distinctly different from that of *E. arvense* [7]. Thus, a LC-UV method to determine each individual aglycone is more appropriate for this determination, facilitating the interpretation of the data obtained in hydrolysis optimization procedure.

3.2.1. LC–UV method validation

A solvent gradient elution system composed of MeOH:H_2O acidified with 0.3% formic acid was selected because it afforded good separation and resolution of the target peaks from their neighboring unknown compound peaks in the *E. giganteum* hydrolyzed extract. The wavelength of 370 nm was selected for the detection of target analytes because it showed good specificity and sensitivity, particularly for quercetin.

The proposed chromatographic method was validated by evaluating the LOD, LOQ, linearity, intra- and inter-day precisions, specificity and accuracy [12]. The resultant calibration curves, LOD and LOQ of flavonoid aglycones are presented in Table 2. The calibration curves were obtained with seven increments of concentrations for standards. Good linearity is shown for both calibration curves.

Under the established experimental conditions, the recoveries of quercetin and kaempferol in the three concentrations levels were in the range of 96.89–103.33% and 98.22–102.49%, respectively. Measurements of these intra- and inter-day precisions for both quercetin and kaempferol yielded good results in the ranges of 0.32–3.13% RSD and 1.05–3.75% RSD, respectively (data not shown). The chromatographic peak purity of the analytes in the hydrolyzed extract was confirmed by analysis with a diode array detector.

The results of the P–B design (Table 3) showed that the method was more susceptible to wide deliberate variation in flow rate (above the usual parameters) and the use of a worn-out column. Care should be taken with these factors whenever the method is applied. The resolution between the quercetin and kaempferol peaks of their neighboring unknown compounds was critical for the results of the robustness test, but even under extreme hydrolysis conditions, where the intensity of the neighboring peaks increased, this method, under normal conditions, proved to be specific for the aglycones of interest.

Table 3
Calculated *t*-values of the factors effects (t_{calc}) on area, retention time (R_t) and peak width of quercetin and kaempferol from results of the P–B design.

Factor	t_{calc}					
	Quercetin peak			Kaempferol peak		
	Area	R_t	Width	Area	R_t	Width
MeOH %	2.05	−9.67[a]	0.65	0.97	−2.00	0.30
Flow rate	−6.65[a]	−11.23[a]	−0.29	−5.35[a]	−4.38[a]	0.00
Formic acid %	1.38	0.07	1.44	0.11	−1.00	0.00
Column	14.75[a]	−2.33	1.91	7.22[a]	−0.24	−2.66[a]
Dummy 1	−0.84	−0.87	−0.75	−0.65	−1.38	−0.89
Dummy 2	1.35	−0.02	−1.21	1.19	−1.02	−0.15
Dummy 3	−0.69	1.50	0.98	−1.08	−0.25	1.48
Critical value	$t_{(0.05,3)}$	2.36				

[a] Significant at 5% level.

3.2.2. Hydrolysis and characterization of flavonoids

Hydrolysis had been previously evaluated using HCl in acetone medium (British pharmacopoeic method), but a low yield of aglycones with a large number of interfering compounds was obtained after the liquid/liquid extraction with ethyl acetate. The replacement of acetone by aqueous methanol improved the yield of aglycones (results not shown). All further experiments were thus carried out with 50% aqueous methanol (v/v), followed by the elimination of methanol and liquid/liquid extraction with ethyl acetate. This procedure allowed the removal of the majority of the interfering compounds, facilitating the quantitative analysis of flavonoid aglycones.

Applying the developed hydrolysis/extraction method to the *E. giganteum* raw material, two flavonol aglycones were observed in the chromatogram and identified as quercetin (R_t=16.1 min, UV λ_{max}=253.4, 295sh, 371.4 nm) and kaempferol (R_t=21.9 min, UV λ_{max}=246sh, 262.9, 292sh, 322sh, 366.6 nm) (Fig. 6).

3.2.3. Hydrolysis optimization

Quercetin and kaempferol aglycones in the hydrolyzed extract of *E. giganteum* (sample 2) were quantified using the developed and validated LC method.

The value of independent variables, the design of experiments through acid hydrolysis and the respective experimental and predicted yield of quercetin and kaempferol are shown in Table 4.

The results obtained for each aglycone (Table 4) were analyzed, and the data were fit to a second-order polynomial model using Eq. (1). The significance of each parameter of the model was evaluated by the *t*-test. In a first analysis, the blocks parameter presented less than 95% significance for kaempferol, but not for quercetin. Thus, due to the low variability in the levels of quercetin, we chose to discard the blocks parameter for both responses. The reduced models were then submitted to an *F*-test (ANOVA) to calculate the significance of the regression (SOR), lack-of-fit (LOF) and the coefficient of multiple determination (R^2).

After regression analysis, a second-order response model was obtained as shown in Eqs. (2) and (3) for quercetin and kaempferol, respectively, and the response surfaces were analyzed and plotted. The models presented significance of the *F*(SOR) higher

Table 4
Experimental conditions, including factors and levels tested, of the central composite rotational design (CCRD), and experimental and predict quercetin and kaempferol yield in acid hydrolysis of *E. giganteum* raw material (sample 2).

Run	Block	Variables				Quercetin yield ($\mu g\ g^{-1}$)[a]		Kaempferol yield ($\mu g\ g^{-1}$)[a]	
		Coded level		Natural variables					
		X_1	X_2	HCl (M)	Time (min)	Experimental	Predicted	Experimental	Predicted
1	1	−1	−1	1.6	60	118	116.7	1585	1568.8
2	1	1	−1	4.4	60	112	111.3	1542	1561.5
3	1	−1	1	1.6	180	147	144.4	2059	2003.5
4	1	1	1	4.4	180	64	62.1	931	911.2
5	1	0	0	3	120	125	125.5	1797	1812.5
6	1	0	0	3	120	127	125.5	1834	1812.5
7	2	−1.4142	0	1.02	120	126	128.1	1646	1689.3
8	2	1.4142	0	4.98	120	65	66.1	919	911.7
9	2	0	−1.4142	3	35.1	127	127.7	1808	1798.2
10	2	0	1.4142	3	204.9	110	112.5	1600	1645.8
11	2	0	0	3	120	125	125.5	1800	1812.5
12	2	0	0	3	120	125	125.5	1819	1812.5

X_1 = HCl molar concentration; X_2 = hydrolysis time.
[a] Yield in $\mu g\ g^{-1}$ of dry weight.

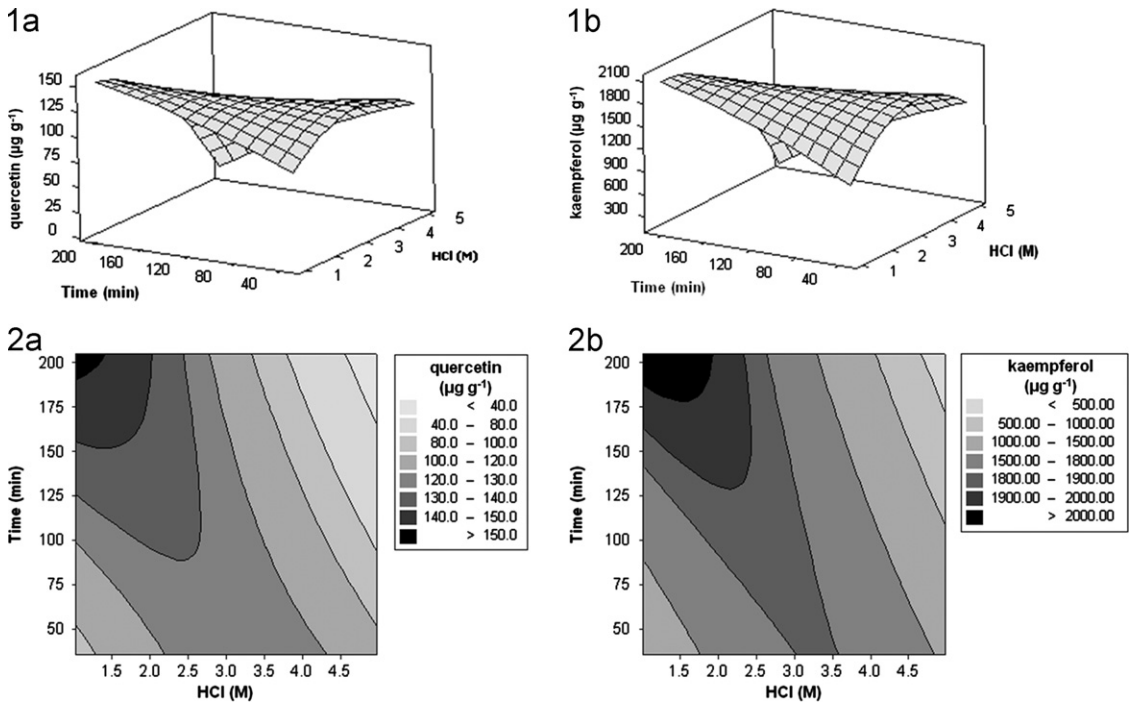

Fig. 5. Response surface (1) and contour plots (2) of HCl molar concentration and hydrolysis time effects on quercetin (a) and kaempferol (b) yield (in $\mu g\ g^{-1}$ of dry plant).

than 95%, significance of F(LOF) lower than 95% and $R^2 > 0.99$

$$\text{quercetin}\ (\mu g\ g^{-1}) = 24.8102 + 55.2823 \times \text{HCl} + 0.776997 \times \text{Time} - 7.23852 \times \text{HCl}^2 - 7.46528\text{E}{-}04 \times \text{Time}^2 - 0.229167 \times \text{HCl} \times \text{Time} \quad (2)$$

$$\text{kaempferol}\ (\mu g\ g^{-1}) = -9.66755 + 974.822 \times \text{HCl} + 11.8059 \times \text{Time} - 130.612 \times \text{HCl}^2 - 0.0125694 \times \text{Time}^2 - 3.22917 \times \text{HCl} \times \text{Time} \quad (3)$$

The contour and three-dimensional (response surface) plots describing the effect of HCl concentration and hydrolysis time on the determination of quercetin and kaempferol in the *E. giganteum* raw material are presented in Fig. 5. In both plots, the interaction between the evaluated factors can be observed, with an improved yield of aglycones from the middle of the run onwards (100 to 204.9 min) and from the lower to the middle level of HCl molar concentration (1.02 to 3 M), i.e., employing a lower acid concentration and longer hydrolysis time at 90 °C.

Both higher HCl concentration and extended hydrolysis time resulted in a decrease in the yield of aglycones, which could be due to their degradation. On the other hand, lower HCl concentration and hydrolysis times might result in the partial hydrolysis of flavonoid glycosides, leading to an underestimation of the flavonoid aglycone content.

From the second-order models, the HCl concentration and hydrolysis time providing the maximum aglycone yield were 1.1801 M and 204.85 min, which predicted quercetin and kaempferol yields of 152 and 2069 $\mu g\ g^{-1}$ of dry drug, respectively. A confirmation experiment was conducted for these predicted optimum conditions (1.18 M HCl and 205 min of hydrolysis, $n=3$). The aglycone yields for *E. giganteum* (sample 2) were

Table 5
Content of total flavonoids, expressed as isoquercitrin (% w/w dry plant), and content of quercetin and kaempferol aglycones (mg g^{-1} dry plant) in *E. giganteum* (sample 2), *E. arvense*, *E. hyemale* and *E. bogotense*.

Assay method	Hydrolysis/extraction method	Results expressed as	*E. giganteum*	*E. arvense*	*E. hyemale*	*E. bogotense*
Spectrophotometry	Pharmacopoeic	Isoquercitrin (%, w/w)	0.66 ± 0.02[a]	1.33 ± 0.01	0.51 ± 0.07	1.10 ± 0.04
	Developed in this work	Isoquercitrin (%, w/w)	1.05 ± 0.06	2.42 ± 0.26	1.01 ± 0.04	1.74 ± 0.05
LC–UV	Pharmacopoeic	Quercetin (mg g^{-1})	0.038 ± 0.003	0.577 ± 0.066	0.016 ± 0.000	0.013 ± 0.000
		Kaempferol (mg g^{-1})	0.375 ± 0.016	0.088 ± 0.012	0.400 ± 0.051	0.494 ± 0.045
	Developed in this work	Quercetin (mg g^{-1})	0.116 ± 0.005	2.313 ± 0.176	0.083 ± 0.002	0.033 ± 0.001
		Kaempferol (mg g^{-1})	1.409 ± 0.061	0.533 ± 0.036	1.380 ± 0.055	2.360 ± 0.063

[a] Value expressed as mean ± standard deviation of three determinations, in terms of dry plant.

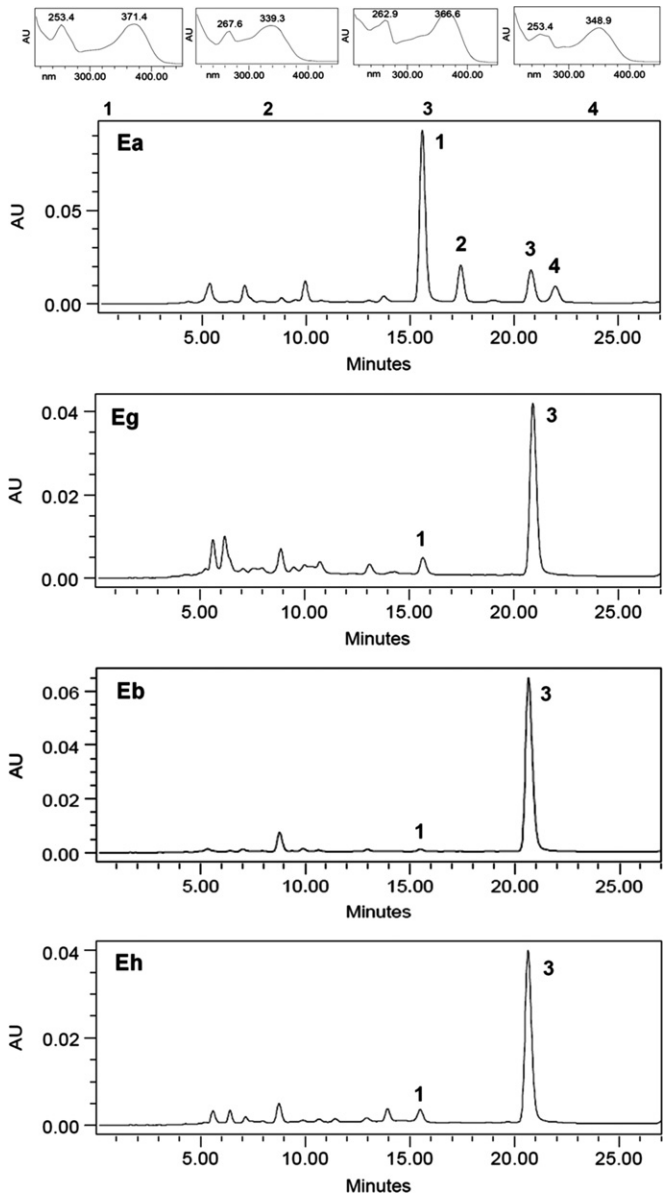

Fig. 6. LC–UV chromatograms at 370 nm of the fraction containing the aglycones of *E. arvense* (Ea), *E. giganteum* (Eg), *E. bogotense* (Eb) and *E. hyemale* (Eh), using the method developed in this work for *E. giganteum*. UV spectra of quercetin (1), apigenin (2), kaempferol (3) and an unknown flavonoid (4).

147 ± 2 μg g^{-1} of quercetin and 1923 ± 11 μg g^{-1} of kaempferol, which were only 3.29% and 7.06% below the predicted values, revealing the good predictivity capacity of the model.

3.3. Aglycone quantification in Equisetum spp.

The optimized hydrolysis conditions obtained for the *E. giganteum* raw material (1.18 M HCl and a hydrolysis time of 205 min at 90 °C in 50% aqueous methanol medium) were employed for the assay of flavonoid aglycones in several *Equisetum* species: *E. giganteum* (sample 2), *E. arvense*, *E. hyemale* and *E. bogotense*. These samples were also submitted to the pharmacopoeic hydrolysis method for *Horsetail* (0.6 M HCl and a hydrolysis time of 30 min under reflux in acetone medium) [10]. The aglycones formed were quantified using the spectrophotometric pharmacopoeic method and the LC–UV method developed and validated in this study. The content of total flavonoids expressed as isoquercitrin and the content of quercetin and kaempferol aglycones were thus obtained (Table 5).

The data presented in Table 5 show that the hydrolysis/extraction method described by the BP2011 [10] yielded lower values of total flavonoids for all four species, including *E. arvense*, compared to those obtained by the application of the hydrolysis/extraction method developed in this study. The contents of total flavonoids were between 58 and 98% higher for the four species compared with levels obtained using the pharmacopoeic method.

In the case of the determination of quercetin and kaempferol aglycones, the samples obtained with the optimized hydrolysis/extraction procedure showed a yield of over 153% for all four species relative to the yield obtained with the extract obtained using the BP2011 method. For *E. arvense*, the contents of quercetin and kaempferol differed by 301% and 506%, respectively, between the content calculated in samples obtained with the optimized hydrolysis/extraction method and the method described in BP2011. These data reveal the influence of the method and hydrolysis conditions in the determination of total flavonoids and aglycones for the four species analyzed, indicating that the glycosilated flavonoids present in these samples are not completely hydrolyzed, which leads to an underestimation of the total flavonoid content.

The increase in the content of quercetin and kaempferol observed by LC–UV after the application of optimized hydrolysis conditions was not proportional to the increase observed using the spectrophotometric method. This difference demonstrates the non-specificity of the spectrophotometric method for aglycone quantitation. Thus, the LC–UV determination of individual aglycones was more specific than the spectrophotometric method, proving to be more appropriate for the quality control of the *Equisetum* species analyzed.

Among these species, *E. arvense* was the only one with a higher content of quercetin than kaempferol, as determined by both hydrolysis/extraction methods. *Equisetum giganteum*, *E. hyemale* and *E. bogotense* exhibited at least 10 times more kaempferol than quercetin. This difference in the levels of these two aglycones may be very useful and perhaps decisive in the differentiation of the analyzed species but also can assist in the identification, mainly for powdered materials in which the botanical identification becomes

difficult and in the quality control of plant material. The initial objective of finding a way to differentiate the species chemically through their aglycone profiles was not achieved, with the exception for *E. arvense*.

For both assay methods, *E. arvense* had the highest content of total flavonoids expressed as isoquercitrin, as well as a higher content of aglycones (considering only quercetin and kaempferol), followed by *E. bogotense*, *E. giganteum* and *E. hyemale*. In addition to having the highest content of aglycones, two other flavonoid aglycones were detected, although not quantified, in the hydrolyzed extract of *E. arvense* (Fig. 6). These compounds can be observed in the chromatogram of *E. arvense*, in which, in addition to quercetin (peak 1, R_t=15.6 min) and kaempferol (peak 3, R_t=20.9 min), there are another two peaks corresponding to apigenin (peak 2, R_t=22 min) and an unidentified flavonoid (peak 4, R_t=17.5 min). In the other three species, only quercetin and kaempferol aglycones were found after the hydrolysis of flavonoid glycosides.

4. Conclusions

The major phenolic compounds of *E. giganteum* were identified for the first time by LC–DAD and LC–MS/MS. Some of these compounds were reported for the first time in the *Equisetum* genus.

Glucosylated kaempferol derivatives proved to be the most abundant flavonoids in *E. giganteum*, showing potential as qualitative and quantitative markers for this species.

Considering that there are no commercial standards available for most flavonoids in the hydroethanolic extract of *E. giganteum*, we developed and validated a reversed phase LC–UV method to determine the flavonoid aglycones content obtained after an optimized hydrolysis process. The developed LC–UV method proved to be simple, sensitive, accurate, linear, precise, reproducible, specific and robust.

When applied to the analysis of flavonoid aglycones in *E. giganteum*, *E. arvense*, *E. hyemale* and *E. bogotense* raw material, the developed hydrolysis method showed higher yields than the method described in BP2011 for *E. arvense* [10]. These results indicate that this method is more suitable for the determination of total flavonoids in *Equisetum* species. Furthermore, it provided the first description of the chromatographic profile and quantification of aglycones in these species.

The results presented in this paper are useful for the differentiation of these *Equisetum* species and represent a contribution to the quality control of *E. giganteum* raw material and derivatives. Additionally, these findings suggest that this method could be extended to other species of the genus *Equisetum*, including *E. arvense*.

Acknowledgments

This work was supported by the Brazilian Agencies CNPq and FAPERGS. CAPES-REUNI provided a doctoral scholarship to the first author. The authors wish to thank F.K.J. Yatsu for excellent discussions and contributions and E. Wilson (Universidad de Belgrano) for assistance with the English language.

References

[1] S. Gorzalczany, A. Rojo, R. Rondinaz, S. Debenedetti, C. Acevedo, Acta Farm. Bonaerense 18 (1999) 221–224.
[2] N.I. Hilgert, J. Ethnopharmacol. 76 (2001) 11–34.
[3] R.M. Pérez Gutiérrez, G.Y. Laguna, A. Walkowski, J. Ethnopharmacol. 14 (1985) 269–272.
[4] A. Cáceres, L.M. Girón, A.M. Martinéz, J. Ethnopharmacol. 19 (1987) 233–245.
[5] J.F. Ovalles, J.R. Fuller, M. Spinetti, Rev. Fac. Farm. 32 (1996) 2–4.
[6] M. Blumenthal, A. Goldberg, J. Brinckmann, Herbal Medicine: Expanded Commission E Monographs, first ed., Integrative Medicine Communications, Newton, MA, 2000.
[7] M. Veit, C. Beckert, C. Höhne, K. Bauer, H. Geiger, Phytochemistry 38 (1995) 881–891.
[8] E.M.Z. Michielin, L.F.V. Bresciani, L. Danielski, R.A. Yunes, S.R.S. Ferreira, J. Supercrit. Fluids 33 (2005) 131–138.
[9] L.N. Francescato, D.A. Quinteros, S. Bordignon, V.L. Bassani, A.T. Henriques, Lat. Am. J. Pharm. 30 (2011) 1196–1201.
[10] British Pharmacopoeia Commission Secretariat, British Pharmacopoeia 2011. Volume IV. Herbal Drugs, The Stationary Office, London, 2011.
[11] B. Domon, C.E. Costello, Glycoconjugate J. 5 (1988) 397–409.
[12] ICH, Validation of Analytical Procedures: Text and Methodology Q2(R1), 2005.
[13] Y. Vander Heyden, A. Nijhuis, J. Smeyers-Verbeke, B.G.M. Vandeginste, D.L. Massart, J. Pharmaceut. Biomed. Anal. 24 (2001) 723–753.
[14] R.H. Myers, D.C. Montgomery, C.M. Anderson-Cook, Response Surface Methodology: Process and Product Optimization Using Designed Experiments, third ed, Wiley, New York, 2009.
[15] M.A. Bezerra, R.E. Santelli, E.P. Oliveira, L.S. Villar, L.A. Escaleira, Talanta 76 (2008) 965–977.
[16] C. Beckert, Biosynthese, Akkumulation und Strukturen von Styrylpyronen in gametophytischen und sporophytischen Geweben von Equisetum in Julius-von-Sachs-Institut für Biowissenschaften, Bayerischen Julius-Maximilians-Universität Würzburg, Würzburg, 2002.
[17] M. Veit, H. Eiger, V. Wray, A. Abou-Mandour, W. Rozdzinski, L. Witte, D. Strack, F.C. Czygan, Phytochemistry 32 (1993) 1029–1032.
[18] B.-J. Park, M. Tomohiko, Chem. Nat. Compd. 47 (2011) 363–365.
[19] L. Jurd, The Chemistry of Flavonoid Compounds, in: T.A. Geissman (Ed.), Macmillan, New York, 1962 (pp. 107–155).
[20] A. Romani, P. Vignolini, L. Isolani, F. Ieri, D. Heimler, J. Agric. Food Chem. 54 (2006) 1342–1346.
[21] F. Ferreres, R. Llorach, A. Gil-Izquierdo, J. Mass Spectrom. 39 (2004) 312–321.
[22] K. Ablajan, Z. Abliz, X.-Y. Shang, J.-M. He, R.-P. Zhang, J.-G. Shi, J. Mass Spectrom. 41 (2006) 352–360.
[23] L. Lu, F.-R. Song, R. Tsao, Y.-R. Jin, Z.-Q. Liu, S.-Y. Liu, Rapid Commun. Mass Spectrom. 24 (2010) 169–172.
[24] B.D. Davis, J.S. Brodbelt, J. Mass Spectrom. 43 (2008) 1045–1052.
[25] R.E. March, E.G. Lewars, C.J. Stadey, X.-S. Miao, X. Zhao, C.D. Metcalfe, Int. J. Mass Spectrom. 248 (2006) 61–85.
[26] F. Vallejo, F.A. Tomás-Barberán, F. Ferreres, J. Chromatogr. A 1054 (2004) 181–193.
[27] C. Medana, F. Carbone, R. Aigotti, G. Appendino, C. Baiocchi, Phytochem. Anal. 19 (2008) 32–39.
[28] M. Veit, K. Bauer, C. Beckert, B. Kast, H. Geiger, F.-C. Czygan, Biochem. Syst. Ecol. 23 (1995) 79–87.
[29] C. Beckert, C. Horn, J.-P. Schnitzler, A. Lehning, W. Heller, M. Veit, Phytochemistry 44 (1997) 275–283.
[30] H. Wiedenfeld, A.A. Cetto, C.P. Amador, Biochem. Syst. Ecol. 28 (2000) 395–397.